Probing Förster Type Energy Pathways in a First Generation Rigid Dendrimer Bearing Two Perylene Imide Chromophores

Tom Vosch,[†] Mircea Cotlet,[†] Johan Hofkens,*[,†] Koen Van Der Biest,[†] Marc Lor,[†] Kenneth Weston,[§,||] Philip Tinnefeld,[§] Markus Sauer,[§] Loredana Latterini,[⊥] Klaus Müllen,[‡] and Frans C. De Schryver*[,†]

Contribution from the Department of Chemistry, Katholieke Universiteit Leuven, Celestijnenlaan 200F, 3001 Heverlee, Belgium, Max-Planck-Institut für Polymerforschung, Ackermannweg 10, 55128 Mainz, Germany, Physikalisch-Chemisches Institut, Universität Heidelberg, Im Neuenheimer Feld 253, 69120 Heidelberg, Germany, and Department of Chemistry, University of Perugia, Via Elce di Sotto, 8, I-06123 Perugia, Italy.

Received: April 7, 2003; In Final Form: June 18, 2003

Ensemble and single molecule spectroscopic measurements on a bichromophoric dendrimer system were performed. Although Förster type energy processes such as energy hopping and singlet−singlet annihilation can be observed at the ensemble and single molecule level, only single molecule measurements can visualize the presence of singlet−triplet annihilation. The flux dependent population of the triplet state suggests facilitated formation of the triplet through a higher singlet excited state. The presence of synthesis inherent structural isomers, not to be distinguished at the ensemble level, could be demonstrated by analyzing modulated fluorescence intensity trajectories. These data show the complementarity of both the ensemble and single molecule approaches in the study of detailed photophysics of a multichromophoric system.

Introduction

Photophysical processes such as energy transfer and energy hopping play a key role in excited-state dynamics of biological multichromophoric systems such as light harvesting complexes[1,2] and oligomeric autofluorescent proteins such as DsRed.[3] Also in conjugated polymers such as polyphenylvinylene (PPV), used in light emitting devices (LEDs), such excited-state dynamics are of importance in their material science applications.[4−8] As a model system to study these photophysical pathways in multichromophoric entities, specially designed rigid dendrimers with a well-defined number of chromophores were synthesized.[9] The chromophores of these dendrimers have a fixed spatial registry through the sp^3 hybridized core and four rigid polyphenylene dendritic arms. In recent publications, the ensemble properties of excited-state processes and decay pathways of similar multichromophoric dendrimers were studied using single photon timing[10] and femtosecond fluorescence upconversion[11] techniques. Using the combination of ensemble and single molecule fluorescence measurements, a better picture of the excited-state processes such as energy hopping, singlet−singlet annihilation, singlet−triplet annihilation, or anion quenching can be established as will be shown in this paper. Therefore, a first generation dendrimer with two chromophores (g1r2) was studied in detail at the ensemble and single molecule level. For comparing some of the properties, also, a dendrimer with one chromophore (g1r1) was studied. The chromophores were attached at the rim of the dendrimer in the para position on the outer phenyl ring. Perylene imide was chosen as chromophore because of its photostability (for a dendrimer system with only one perylene imide chromophore we find an average value of 1.5×10^6 emitted photons assuming a detection efficiency of 10%),[12] its absorption wavelength (around 500 nm), its molar extinction coefficient (38 000 M^{-1} cm^{-1} at 490 nm in toluene), and its high fluorescence quantum yield ($\Phi_f = 0.95$ in toluene).[12]

Materials and Methods

Materials. The synthesis of the rigid dendrimers with one (g1r1) and two (g1r2) perylene imide chromophores has been published separately.[9]

Steady-State Spectroscopy. Steady-state absorption and fluorescence spectra were recorded on a Lambda 40 spectrophotometer (Perkin-Elmer) and Fluorolog-3 fluorimeter (ISA instruments Jobin Yvon-SPEX), respectively. The dendrimers were dissolved in toluene (Aldrich) to have an optical density of about 0.1 in a 1 cm cuvette at the absorption maximum (490 nm), which corresponds to a concentration of 2.5×10^{-6} M.

Triplet Absorption Measurements. The recording of the triplet absorption spectrum was done using acetonitrile, benzene, and toluene (Fluka, spectroscopic grade) as solvents without further purification. The ns-transient absorption measurements were performed on the setup previously described.[13] The direct excitation of the samples at 460 nm was carried out using the output of an Optical Parametric Oscillator (OPO, $\lambda_{exc} = 460$ nm, pulse width ca. 7 ns, energy ca. 1.0 mJ/pulse Continuum) which was pumped by the third harmonic of a Nd:YAG laser. In the sensitization experiments, the samples were excited at 355 nm using the output of the third harmonic of a Nd:YAG laser ($\lambda_{exc} = 355$ nm, pulse width ca. 5 ns, energy ca. 1.5 mJ/pulse, Continuum). Triplet transient absorption spectra were constructed based on measurements every 10 nm over the 300−800 nm spectral range, averaging at least 10 shots per recorded

* To whom correspondence should be addressed. E-mail: Frans.Deschryver@chem.kuleuven.ac.be, Johan.Hofkens@chem.kuleuven.ac.be.
[†] Katholieke Universiteit Leuven.
[‡] Max-Planck-Institut für Polymerforschung.
[§] Universität Heidelberg.
[||] Current address: the Department of Chemistry and Biochemistry, Florida State University, FL 32306.
[⊥] University of Perugia.

10.1021/jp034906d CCC: $25.00
Published on Web 08/14/2003

wavelength. The triplet−triplet molar extinction coefficients (ϵ_T) were determined by the energy transfer method using benzophenone (Aldrich, gold label) and fluoren-9-one (J. T. Baker Chemicals, Photosensitizers Kit) as triplet energy donors.[14] The triplet quantum yield (Φ_T) was calculated from the experimental values of $\Phi_T\epsilon_T$ and ϵ_T. The product $\Phi_T\epsilon_T$ for each compound was obtained by the laser energy effect on the change of absorbance (ΔA) measured at the λ_{max} for the samples under investigation and using an optically matched solution of benzophenone in acetonitrile ($\Phi_T\epsilon_T = 6500\ M^{-1}cm^{-1}$). The plots of ΔA vs laser dose were linear and passed through zero indicating that only one-photon processes were occurring. The error on ϵ_T was estimated to be 20%.

Singlet and Radical Anion Transient Absorption Measurements. The transient absorption measurements were done by femtosecond polychromatic transient absorption. The amplified femtosecond double OPA laser system has been described in detail previously.[15] Briefly, one-half of the output of the regenerative amplifier was used in one OPA to generate the excitation pulse of the appropriate wavelength, the other half served for generation of a fs white light continuum for probing the absorption changes. This fs white light continuum was generated in a 3.1 mm sapphire plate. The actual detection was done by a 256-lines CCD camera (EEV 30, Princeton Instruments) mounted at the exit of a 30 cm spectrograph (SP300i, Acton Research). All compounds were dissolved in THF and MeTHF at a concentration that yielded an absorption of ca. 0.4 in a 1 mm quartz cell at the excitation wavelength of 495 nm (no flow was applied on the sample). To avoid photodegradation of the compounds, the experiments were performed at low excitation fluxes (an average value $<1.2\ \mu W/mm^2$). Errors on the epsilon values of the singlet absorption and anion radical absorption spectra were estimated to be 25%.

Single Molecule Measurements. Samples for single molecule measurements were prepared by spin-coating solutions of g1r1 and g1r2 ($\sim 10^{-10}$M) in toluene containing 10 mg/ml zeonex ($T_g = 132$ °C) or 10 mg/mL PMMA on a carefully cleaned cover glass at 1500 rpm. For the detection of the individual molecules, an Olympus IX 70 inverted microscope equipped with a scanning stage (Physics Instruments, Waldbronn, Germany) was used. Excitation with 488 nm pulsed laser light (8.13 MHz repetition rate, pulse width 1.2 ps) occurred through an oil immersion objective (Olympus 1.4 N. A., 100×). Fluorescence that was collected by the same objective, passed through a dichroic mirror (Chroma Technology, Brattleboro, NY), was filtered through a notch filter (Kaiser Optical Systems, Ann Arbor, MI) and focused via a 50-μm pinhole on an avalanche photodiode (SPCM 15, EG & G, Quebec). The average power of the excitation light before entering the microscope was 0.3 μW. After parking an individual molecule in the laser focus, the fluorescence signal detected by the APD was registered by a time correlated single-photon counting personal computer card (SPC 630, Picoquant, Berlin) by using a modified burst-integrated fluorescence lifetime (BIFL) technique.[16,17] For each detected photon, the time position with respect to the excitation pulse and the time lag with respect to the previous detected photon are stored. The BIFL type data set allows the reconstruction of the fluorescence intensity trajectories (transient) with a user defined dwell time, as well as the time-resolved fluorescence decays by using photons belonging to particular regions of the transient, i.e., regions of constant intensity. The reconstructed fluorescence decays were analyzed by a least-squares method or a maximum likelihood estimation (MLE) method depending on the integrated amount of counts in the decay, convoluting the experimental instrumental response function (full width half-maximum of 400 ps) with an exponential model function containing a time shift, a baseline for the uncorrelated background, and a scaling factor for the correlated background.[18] For the fluorescence intensity trajectories and the coincidence measurements, a classical Hanbury-Twiss and Brown type of setup (coincidence setup) in combination with pulsed excitation was used.[19] For this purpose a 50/50 nonpolarizing beam splitter was added in the detection part such that the fluorescence was focused in 2 APD detectors. A time-to-amplitude converter (TAC) measured the time intervals between photons (one detector channel is the start, and the other is the stop). Because we use pulsed excitation light, the histogram of the interphoton arrival times is determined by the laser repetition rate (8.13 MHz, or intervals of 123 ns), because the interphoton arrival times can only be multiples of the repetition frequency. To compensate for the dead time of the SPC 630 card, a delay was added before one detector.[19] The excitation power before entering the microscope was 1.5−2 μW. One can calculate (vide infra) that applying 2 μW at the single molecule level leads to a large number of two excitations per pulse.

The absorption cross section (σ) of g1r2 is $3.82 \times 10^{-21}\epsilon$ in cm^2 or $\sigma = 2.9 \times 10^{-16}\ cm^2$ ($\epsilon = 76\ 000 M^{-1}cm^{-1}$ at 480 nm). 2 μW average power or 2×10^{-6} J/s corresponds needs to be divided by 8.13×10^6 pulses/s to know the energy per pulse (2.46×10^{-13} J/pulse). One photon of 488 nm has an energy of 4.1×10^{-19} J. So there are 6×10^5 photons per pulse. The diffraction limited spot has a surface of $3.1 \times 10^{-10}\ cm^2$ resulting in a density of 1.94×10^{15} photons/cm^2. Multiplying 1.94×10^{15} photons/cm^2 with $\sigma = 2.9 \times 10^{-16}\ cm^2$ gives a value of 0.561. Thus, the probability of one excitation per pulse is 0.561, whereas the probability for two excitations per pulse is 0.561(0.558/2) = 0.16 (one needs to divide by two because when one photon is absorbed, the absorption cross section is only half the original value). Multiplying this value with 8.13×10^6 and dividing with 10 (10% detection efficiency) results in 122 700 double excitation events, assuming no intersystem crossing.

The fluorescence spectra were measured with a liquid-nitrogen-cooled, back-illuminated CCD camera (LN/CCD-512SB, Princeton Instruments) coupled to a 150-mm polychromator (SpectraPro 150, Acton Research Cooperation) using a 10 s integration time. The recorded spectra were corrected for the background, the response of the CCD camera, and the optics used. Determination of the peak position within accuracy of 1 nm of each spectrum was done by calculating the first and second derivatives. All measurements were carried out at room temperature.

Calculations of Triplet Lifetime and Rate Constant of Intersystem Crossing. The analysis of the triplet lifetimes in all recorded fluorescence intensity trajectories in PMMA and of the recorded fluorescence intensity trajectories in zeonex under nitrogen atmosphere was performed by building up the second-order intensity correlation (autocorrelation traces) from the fluorescence intensity trajectories binned to 50 μs.[20] The autocorrelation trace had 200 channels and was fitted with a single-exponential decay model. The rate constant for intersystem crossing (k_{ISC}) was estimated from the fluorescence intensity trajectories rebinned to 0.5 ms and using eq 1[21]

$$k_{ICS} = \frac{\xi}{\tau_{on} I_{fl} \tau_{fl}} \tag{1}$$

where ξ is the detection efficiency of the setup, τ_{on} is the on

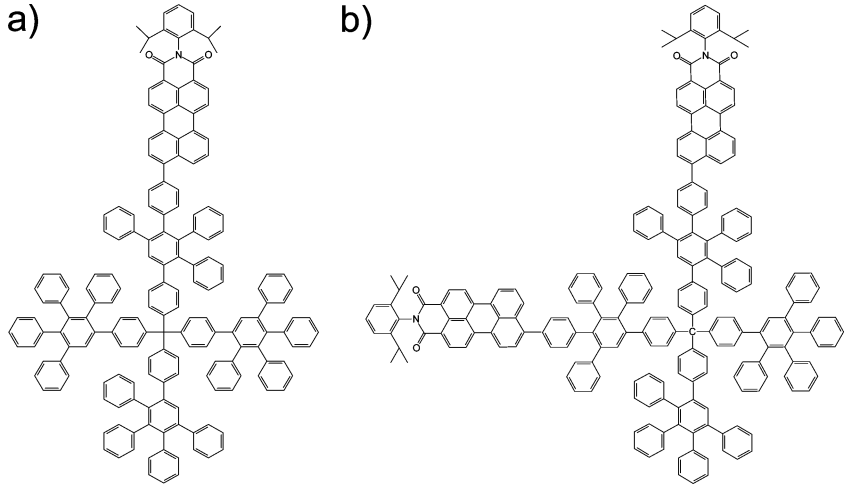

Figure 1. Chemical structures of (a) g1r1 and (b) g1r2.

time, I_{fl} is the fluorescence intensity of the signal (in counts per second), and τ_{fl} is the fluorescence lifetime. The product $\tau_{on}I_{fl}$ was estimated as the number of detected photons (corrected for the background signal) divided by the number of off events (eq 2)

$$\tau_{on}I_{fl} \approx \frac{\text{number of detected photons}}{\text{number of off events}} \tag{2}$$

Calculations of the Angle between the Chromophores and the Structural Isomers of g1r2. The modulated fluorescence intensity traces (MFITs) were recorded by rotating the direction of the polarization of the excitation light using a half wave plate with a frequency of several Hertz. The MFITs from single g1r2 molecules were fitted to a cosine square function in Origin 6.0 using Levenberg−Marquardt iterations that are implemented in the program using eqs 3 and 4 to fit respectively the second and first level of the fluorescence intensity[22−24]

$$y = \text{b1}\cos^2(wx + p_b) + \text{bg} \tag{3}$$

$$y = a\cos^2(wx + p_a) + \text{b2}\cos^2(wx + p_b) + \text{bg} \tag{4}$$

b1 and b2 are the amplitudes of the longest surviving chromophore, where a is the amplitude of the first bleached chromophore. w is the modulation frequency, p_b and p_a are the phase difference between the transition dipole moment of the respectively longest and shortest surviving chromophore and the direction of linear polarized excitation light at the beginning of the experiment, and bg is the background signal. The difference between p_b and p_a yields the projection of the angles between the two chromophores in the experimentally observed $X-Y$ plane. As in a $\cos^2$ function, the arguments α, $\pi-\alpha$, $\pi+\alpha$, and $2\pi-\alpha$ are equivalent, all results were projected into the interval [0°,90°]. To compare our experimentally obtained histogram of angles, Monte Carlo simulations of random projections of the angles between the chromophores in the different structural isomers of g1r2 in a fixed $X-Y$ plane were done using a self-written C-program. The structural isomers were obtained by molecular geometry optimization using the Merck Molecular Force Field (molecular mechanics method) imbedded in Spartan 5.

Results and Discussion

Ensemble Spectroscopy. Chemical structures of g1r1 and g1r2 are given in Figure 1, parts a and b, respectively. Stationary absorption and fluorescence measurements in toluene were performed at room temperature. The corresponding spectra for g1r1 (line with triangles) and g1r2 (line with squares) are presented in Figure 2a. The maxima in the absorption spectrum are situated at 495 and 521 nm, respectively, whereas the maximum of the emission spectrum is found at 557 nm. The quantum yield of fluorescence of both g1r1 and g1r2 in toluene is 0.98. The fluorescence decay of g1r2 measured in toluene at room temperature using 488 nm excitation laser light and detection at 600 nm is single exponential with a decay time of 4.0 ns. As can be seen in Figure 2a, the absorption and emission properties of g1r2 are identical to that of g1r1 indicating the absence of strong coupling of the chromophores in the ground state. When two fluorescent chromophores are in close proximity (2−10 nm range) and there is a weak interaction between their transition dipole moments, the Förster model is applicable.[25] Förster showed that this can lead to Förster resonant energy transfer (FRET), a process that involves the transfer of excitation energy from a donor to an acceptor of two weakly coupled transition dipole moments.[25] Within the Förster formulation, the rate constant of FRET can be expressed as

$$k_{ET} = \left(\frac{R_0}{R}\right)^6 k_D \tag{5}$$

R is the interchromophoric distance. k_D is the inverse of the decay time of the donor. R_0 (the Förster radius) is the distance at which efficiency equals 50%, i.e., the distance at which an equal probability exists for the excited chromophore to relax to the ground state or to undergo energy transfer. R_0 depends on the relative orientation of the transition dipoles toward each other (κ^2) and the spectral overlap ($J(\lambda)$) of the absorption spectrum of the acceptor and the emission spectrum of the donor as can be seen in eq 6.[26] Φ_D represents the quantum yield of fluorescence of the donor, and n is the refractive index of the solvent

$$R_0 = 0.211(\kappa^2 n^{-4}\Phi_D J(\lambda))^{1/6} \tag{6}$$

For a rigid bichromophoric system like the one investigated here, the distance and orientation of the chromophores are constant and hence the rate constant will be determined by the spectral overlap of the donor and acceptor. Moreover, because of the inherent overlap of absorption and emission at room temperature, FRET can occur also between identical chromophores, a process that is known in the literature as energy hopping or homo-FRET.

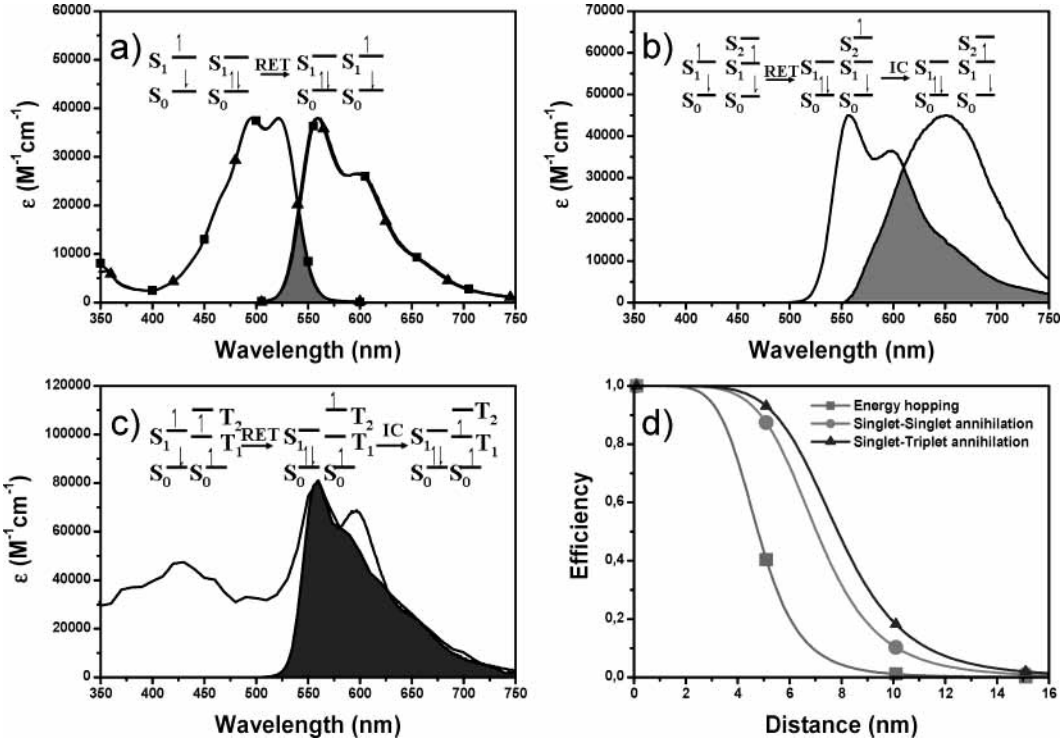

Figure 2. (a) Stationary absorption and emission spectra of g1r1 (line with triangles) and g1r2 (line with squares) in toluene. The spectral overlap is the shaded area. Inset: energetic scheme accounting for energy hopping (b) Transient absorption (S_1-S_n) and emission spectra of g1r2 in toluene. The spectral overlap is the shaded area. Inset: energetic scheme accounting for singlet−singlet annihilation. (c) Triplet absorption and emission spectra of g1r2 in toluene. The spectral overlap is the shaded area. Inset: energetic scheme accounting for singlet−triplet annihilation. (d) Schematic picture of the efficiency as a function of distance for the three Förster-type processes that are present in g1r2.

However, FRET is not restricted to the nonradiative transfer of energy from a donor in the excited state to a ground-state acceptor. Transfer processes that are allowed within the Förster formalism are those for which there are no changes in electron spin in the acceptor transition. Therefore, even energy transfer processes between the donor and acceptor molecule with different spin multiplicity are likewise possible. Hence, the transfer of excitation energy from a chromophore residing in the first excited singlet state to another chromophore residing either in an excited singlet state or in an excited triplet state are possible and are competitive energy transfer pathways. Those two processes are known in the literature as singlet−singlet annihilation and singlet−triplet annihilation, respectively. Hence, several scenarios for FRET are possible and will be discussed in detail.

(1) Direct excitation of one of the chromophores in g1r2 can lead to fluorescence or nonradiative internal conversion (IC) to the ground state or to energy hopping to a neighboring chromophore. Energy hopping is possible in g1r2 and can be seen in Figure 2a where the spectral overlap of the emission spectrum of the donor and the absorption spectrum of the acceptor is given. Energy hopping can be experimentally determined by single photon timing experiments. Time-resolved fluorescence depolarization experiments of g1r2 show a biexponential anisotropy fluorescence decay with values of 1.72 and 0.09 ns. The 1.72 ns can be associated to a rotational correlation decay time of the whole dendrimer, whereas the fast depolarization decay time of 0.09 ns can be related to excitation energy hopping among the identical perylene imide chromophores. A value of 0.09 ns corresponds to a rate constant of energy hopping (k_{ET}) of 5.2×10^9 s^{-1}.[10] For the g1r1 only, a monoexponential decay with a value of 1.4 ns is found for the time-resolved fluorescence depolarization experiments which can be associated to a rotational correlation decay time of the whole dendrimer.[10] Taking into account the spectral overlap given in Figure 2a and a κ^2 of 1.92 we can calculate a R_0 value of 4.78 nm for the energy hopping process. This κ^2 value is an average value, based on the orientations of the chromophores that was computed from molecular mechanics calculations of eight structural isomers of g1r2 (vide infra). These molecular mechanics calculations give an average interchromophoric distance for g1r2 of 2.6 nm. Based on the experimentally obtained R_0 value, k_{ET} and k_D and using eq 5 we find an interchromophoric distance of 2.88 nm which is in good agreement with the value of 2.6 nm that is found by performing molecular mechanics calculations. The process of energy hopping has an efficiency (E_{ff}) of 97.5% based on eq 7

$$E_{ff} = \frac{{R_0}^6}{{R_0}^6 + R^6} \tag{7}$$

(2) If the bichromophoric system undergoes optical excitation under high photon flux, two excited states (S_1) can be present in a single g1r2 molecule at the same time. If the S_1-S_0 transition of one chromophore is in resonance with a transition of S_1 of the other chromophore to a higher excited singlet states, i.e., a S_1-S_n transition, energy transfer between the excited singlet states can occur. The process results in only one excited-state remaining in the bichromophoric system and is often referred to as singlet−singlet annihilation. As depicted in Figure 2b, there is a large overlap between the S_1-S_n absorption spectrum (the singlet absorption spectrum was measured by femtosecond transient absorption measurements) and the fluorescence spectrum which leads to an R_0 value of 7.04 nm for this process. Hence, if a high photon flux is applied on this bichromophoric system, this process can occur with an efficiency of 99.7% based on an interchromophoric distance of 2.6 nm. The presence of this process was proven before at the ensemble

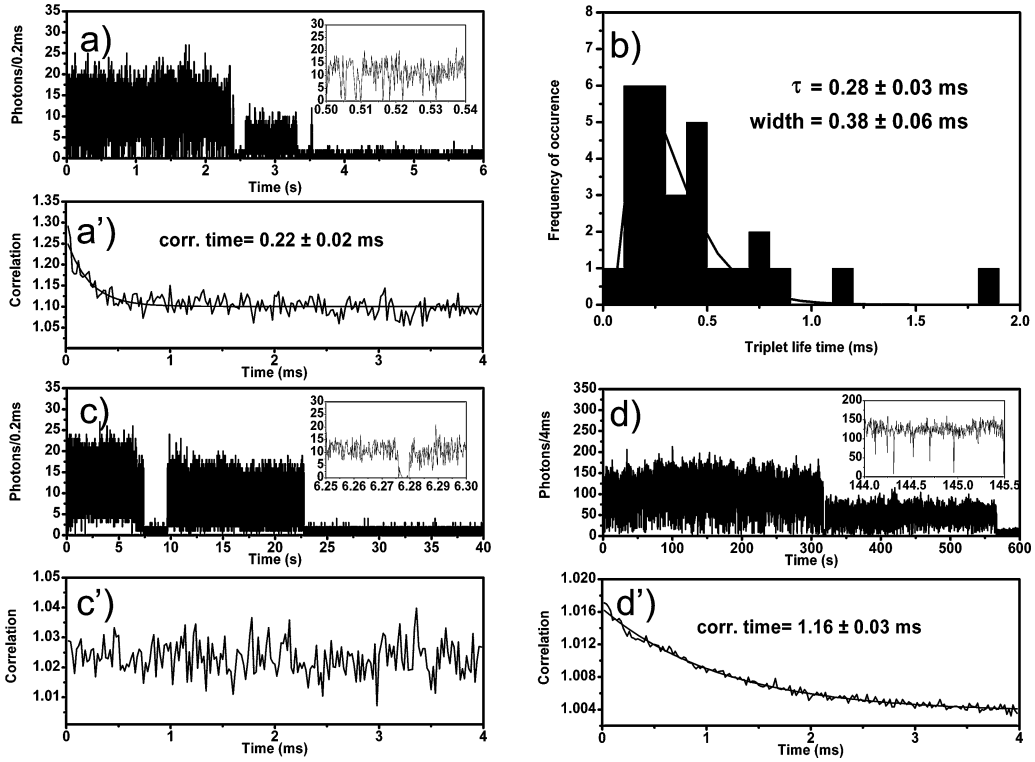

Figure 3. (a and a′) Fluorescence intensity trajectory of a g1r2 molecule embedded in a PMMA polymer matrix together with the autocorrelation trace using pulsed excitation and normal atmospheric conditions. (b) Histogram and a Poisson fit of all the triplet lifetimes of 28 molecules of g1r2 in PMMA using pulsed excitation and normal atmospheric conditions. (c and c′) Fluorescence intensity trajectory of a g1r2 molecule embedded in a zeonex polymer matrix together with the autocorrelation trace using pulsed excitation and normal atmospheric conditions. (d and d′) Fluorescence intensity trajectory of a g1r2 molecule in zeonex together with the autocorrelation trace using pulsed excitation and working under a nitrogen atmosphere.

TABLE 1: Overview of the Triplet Lifetime and Rate Constants for Intersystem Crossing for g1r1 and g1r2 in Zeonex and PMMA under Continuous Wave and Pulsed Excitation

compound	polymer	exc. cond.	$\tau_{triplet}$ atm (ms)	$\tau_{triplet}$ N_2 (ms)	k_{ISC} atm (s^{-1})	k_{ISC} N_2 (s^{-1})
g1r1	pmma	pulsed	0.37 ± 0.02	1.40 ± 0.05	7500	8700
g1r1	pmma	CW	0.29 ± 0.01	*a*	4700	*a*
g1r1	zeonex	pulsed	*b*	1.05 ± 0.03	*b*	6000
g1r1	zeonex	CW	*b*	1.15 ± 0.29	*b*	4000
g1r2	pmma	pulsed	0.28 ± 0.03	1.26 ± 0.06	10000	20200
g1r2	pmma	CW	0.27 ± 0.02	*a*	4800	*a*
g1r2	zeonex	pulsed	*b*	1.21 ± 0.05	*b*	23200
g1r2	zeonex	CW	*b*	1.14 ± 0.18	*b*	4800

[a] Value not measured. [b] No values could be determined due to fast quenching by oxygen.

level by means of femtosecond fluorescence upconversion and time-resolved polychromatic femtosecond transient absorption measurements.[11,27,28]

(3) Besides the previously mentioned possibilities, direct excitation of one of the chromophores can lead also to intersystem crossing (ISC) to the triplet state. Because of the relatively long lifetime of the triplet state, the second chromophore can be excited so that two excited states can be present in a g1r2 molecule, a S_1 and a T_1 state. If the triplet state exhibits transitions into higher excited triplet states, T_n, that are in resonance with the $S_1 \rightarrow S_0$ transition, singlet−triplet energy transfer, i.e., energy transfer from the excited singlet state to the energetically lower lying triplet state, can occur.[29] This process is often called singlet−triplet annihilation, as the net result is one excited state in the bichromoporic system, in this case a triplet state. Such a process however cannot be directly observed by ensemble measurements because fluctuations in fluorescence intensity caused by this off process will be masked by averaging over a large number of emitting molecules. Using single molecule measurements, one gets rid of the averaging effect, and the collective off's because of the singlet−triplet annihilation in the fluorescence intensity trajectories can be observed. Based on triplet transient absorption measurements, a Förster radius of 7.86 nm was calculated (see Figure 2c for the spectral overlap of the triplet absorption spectrum and the singlet emission spectrum). Based on this R_0 value of 7.86 nm and interchromophoric distance of 2.6 nm, we find an efficiency of this process close to 100 percent. In Figure 2d, the efficiencies of the three Förster-type processes are given as a function of distance for g1r2.

Single Molecule Fluorescence Intensity Traces. Figure 3a shows an example of a fluorescence intensity trajectory of a g1r2 molecule embedded in a PMMA polymer film using 488 nm pulsed excitation light. Two stable fluorescence intensity levels are detected. When one chromophore is bleached, it does not act as a quencher, otherwise we would not observe two fluorescence intensity levels.[12] Analysis of the off times shows that three different off processes are present. The shortest of these three processes is attributed to triplet blinking. This process related to triplet formation can be seen in the zoom in Figure

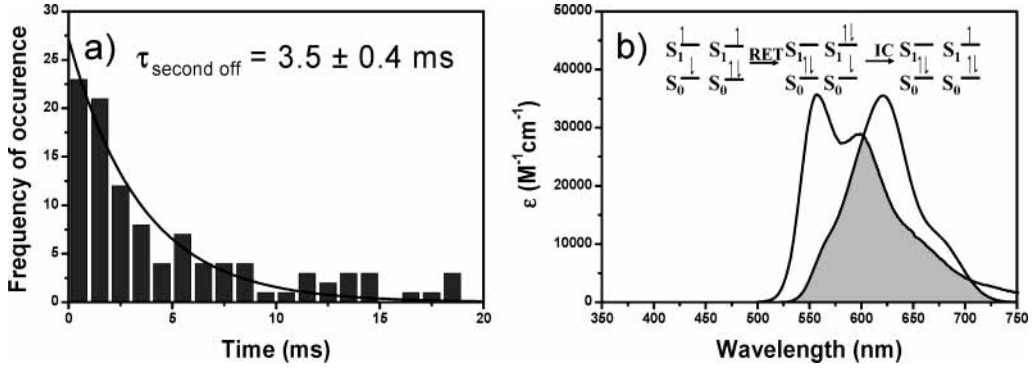

Figure 4. (a) Histogram and exponential fit of off times of 105 off events from 30 different g1r2 molecules in zeonex under normal atmospheric conditions. (b) Perylene imide anion radical absorption spectrum and g1r2 emission spectrum in toluene. The shaded area represents the spectral overlap of the anion quenching process.

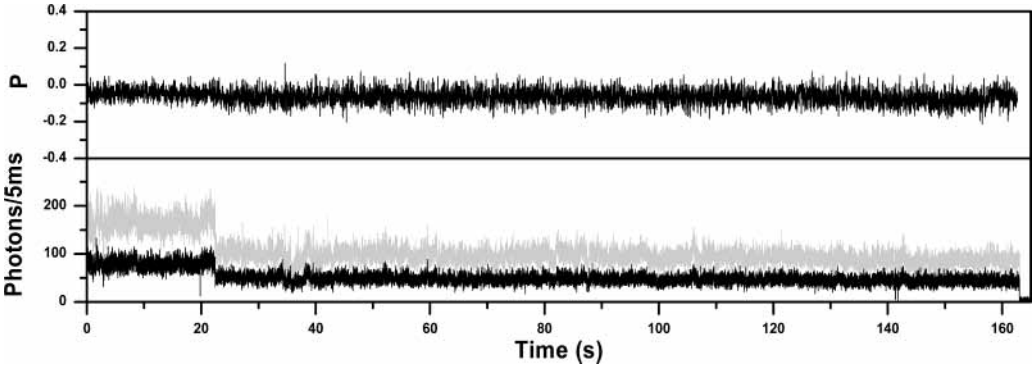

Figure 5. Fluorescence intensity trace of a single g1r2 molecule together with *p*-value trace. The parallel component is depicted in gray, whereas the perpendicular component is depicted in black.

3a and shows up in the autocorrelation trace as a process with a correlation time of 0.22 ms. A total of 29 molecules were analyzed, and from the obtained results, a histogram was constructed and fitted with a Poisson function as can be seen in Figure 3b. From this, an average value for the triplet lifetime of g1r2 in PMMA of 0.28 ms is obtained. Changing the polymer matrix to zeonex has a large impact on the lifetime of the triplet as can be seen in Figure 3c. Here also a g1r2 molecule is represented, but no offs related to the triplet are visible in the fluorescence intensity trajectory. Also the autocorrelation trace shows that there is no correlation in this time domain. However, when nitrogen is flowed over the same sample, the off process related to the triplet formation appears again as can be seen in Figure 3d. After analyzing the autocorrelation traces from 37 recorded molecules and fitting the histogram of the recovered triplet lifetimes, an average value of 1.21 ms for it is obtained. The absence of this fast process in zeonex in the presence of oxygen is due to efficient quenching by oxygen because zeonex has a higher permeability for oxygen than PMMA.[30] This is also confirmed by measurements of g1r2 in PMMA under a nitrogen environment that give a value of 1.26 ms for 28 molecules indicating that the removal of oxygen lengthens the triplet lifetime to a value that is similar to the value obtained in zeonex.

An overview of all of the triplet lifetimes recovered under various conditions is given in Table 1. Similar to g1r2, experiments under pulsed excitation were done for g1r1. Here only one stable fluorescence intensity level was found. For the g1r1 in PMMA under normal atmosphere a value of 0.37 ms was found for the triplet lifetime (average value based on 26 molecules). This value is similar to the value found for g1r2. Values of 1.4 and 1.05 ms, respectively, were found (average values are based on 26 and 33 molecules), for g1r1 measured under nitrogen in PMMA and in zeonex, and these are similar as those found for g1r2 under nitrogen atmosphere. Besides an investigation of the triplet lifetime, also the rate constants of intersystem crossing were determined by using a threshold method on the fluorescence intensity trajectories binned to 0.5 ms. The rate constant values for intersystem crossing that were found are given in Table 1. These values for the rate constant of intersystem crossing range from 6000 up to 23 200 s^{-1} under different experimental conditions and for different compounds. Moreover, the excitation conditions were changed from pulsed to continuous wave excitation. For the triplet lifetime of g1r1 and g1r2 in PMMA, values of 0.29 and 0.27 ms were found, respectively (average values are based on 24 and 65 molecules, respectively). When changing to a nitrogen only atmosphere in zeonex, values for the triplet lifetime of 1.15 ms for g1r1 (based on 12 molecules) and 1.14 ms for g1r2 (based on 9 molecules) were found. The recovered rate constants of intersystem crossing under different experimental conditions and for different compounds using continuous wave excitation range from 4000 to 4800 s^{-1} can be seen in Table 1. We can conclude that the triplet lifetime values are similar to those found under pulsed excitation. Under normal atmospheric conditions a triplet lifetime of about 0.3 ms was found for g1r1 and g1r2 in PMMA using continuous wave or pulsed excitation. Under nitrogen atmosphere, a value of about 1.2 ms was found for g1r1 and g1r2 in PMMA and zeonex using continuous wave or pulsed excitation. Based on all of the calculated intersystem crossing rates that are represented in Table 1, we argue that the rate constant of intersystem crossing under pulsed excitation in multichromophoric dendrimers is significantly larger. This indicates that at a high photon flux a multiphoton process is present that enhances the rate constant of intersystem crossing 3- to 6-fold. An increase in the intersystem crossing rate up to

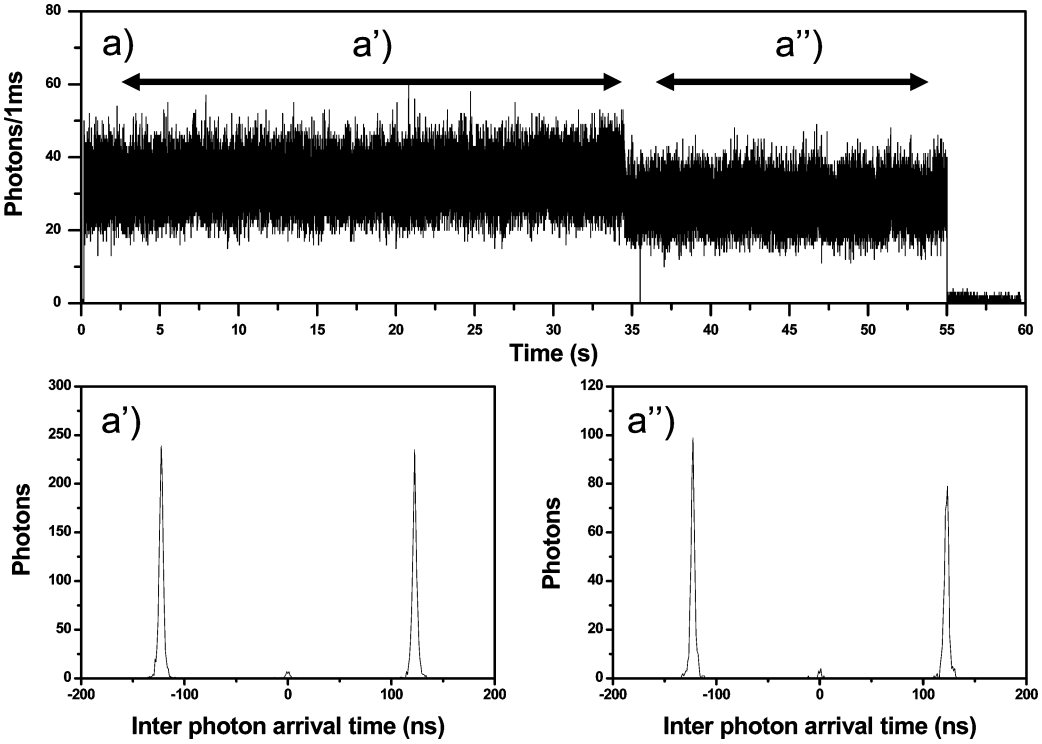

Figure 6. (a) Transient of a compound 2 molecule in zeonex, together with the coincidence graph of the first (a′) intensity level and the second (a″) intensity level. (a) Transient of a compound 2 molecule in zeonex, together with the coincidence graph of the first (a′) intensity level and the second (a″) intensity level.

46 000 s^{-1} was also confirmed for a similar dendrimer as g1r2 but bearing 4 chromophores (g1r4) in PMMA under nitrogen atmosphere. It might be that singlet−singlet annihilation in a multichromophoric dendrimer leads to a high energetic singlet state from which there is a higher probability to go the triplet state then to the relaxed S_1 state.

The two other off processes that are present are demonstrated in Figure 3c. Here we see in the zoom around 6.28 s in the fluorescence intensity trajectory an off event that lasts 5 ms and an off event around 7.5 s that lasts almost 2 s. The nature of these two processes is not fully understood, but we suggest that the one in the millisecond range might be related to the formation of a radical anion. It is possible that one of the chromophores in g1r2 forms a radical anion which can act as a trap for the fluorescence of the other chromophore resulting again in a collective off behavior of the g1r2 molecule. The radical anion acts as an acceptor and is excited to a higher excited state whereas the other chromophore returns to the ground state. Then the radical anion relaxes back to its lowest state by internal conversion. Figure 4b shows the overlap of the radical anion absorption spectrum and the fluorescence spectrum together with a scheme of this process. Based on the overlap of the anion absorption spectrum (obtained from a similar dendrimer with a triphenylamine as core instead of a carbon sp^3 atom) and the steady-state emission spectrum, a Förster radius of 5.60 nm was calculated for this process.[31] The reason we argue that this second millisecond off process is different from the triplet off process is that in the fluorescence intensity trajectories under normal atmosphere in zeonex we see only a few off events in the millisecond region. From the results obtained under nitrogen atmosphere, we know that the triplet should have a higher quantum yield of triplet formation. Taking into account that zeonex is more permeable for oxygen than PMMA, the triplet lifetime should therefore be shorter than the value found for PMMA (about 0.3 ms, see Table 1), and therefore, we can exclude that these millisecond off events in zeonex under normal atmosphere are related to triplet blinking. The perylene imide chromophore has a reduction potential and an oxidation potential with respect to a standard calomel electrode of −1.10 and +1.37 V, respectively.[32] A redox reaction with an oxidizable site in the polymer matrix might create the anion.

TABLE 2: Overview of the Second off Time for g1r1 and g1r2 in Zeonex under Continuous Wave and Pulsed Excitation under Normal Atmospheric Conditions

compound	polymer	exc. cond.	2nd off time (ms)
g1r1	zeonex	pulsed	3.50 ± 1.5
g1r1	zeonex	CW	2.00 ± 0.4
g1r2	zeonex	CW	3.50 ± 0.4
g1r2	zeonex	pulsed	5.00 ± 1.5

The histogram of all the off events (105 events) related to the process in the several millisecond range for g1r2 in zeonex using continuous wave excitation is given in Figure 4a. Fitting the histogram with an exponential decay, a value of 3.5 ms was obtained (see Table 2). For pulsed excitation, a similar value of 5 ms (128 events) was obtained. An indication that this indeed might be the anion radical comes from nanosecond transient absorption measurements that show a lifetime of several milliseconds for the anion radical of a similar first generation polyphenylene dendrimer with a triphenylamine core and one perylene imide chromophore at the rim.[33] For g1r1, a value of 2 (42 events) and 3.5 ms (37 events) was found in zeonex for continuous wave and pulsed excitation, respectively. In PMMA, we did not analyze this second off process because it is not possible to discriminate it from the triplet off process. We can therefore not comment on the question if it is only present in zeonex or if it also is present in PMMA. Also it is not possible to determine whether it depends on the presence of oxygen because if we work under a nitrogen environment, we cannot discriminate the triplet off process from the second off process.

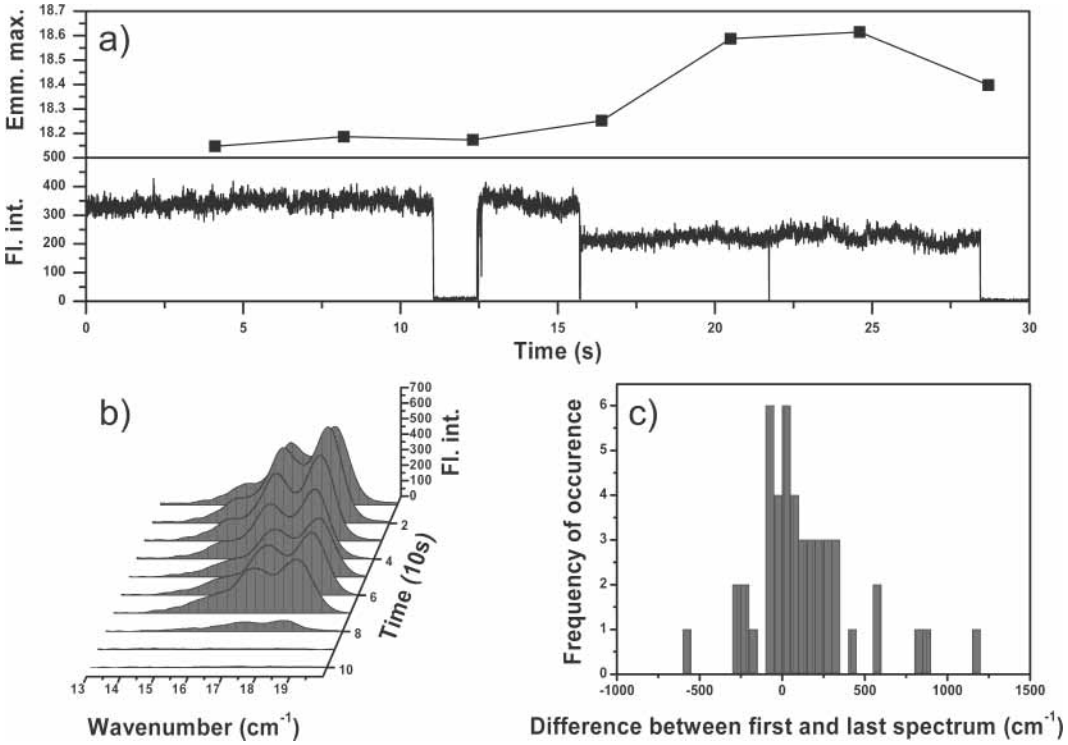

Figure 7. (a and b) Fluorescence intensity trace together with spectral run of an individual g1r2 molecule. (c) Histogram of the range of spectral fluctuations on g1r2.

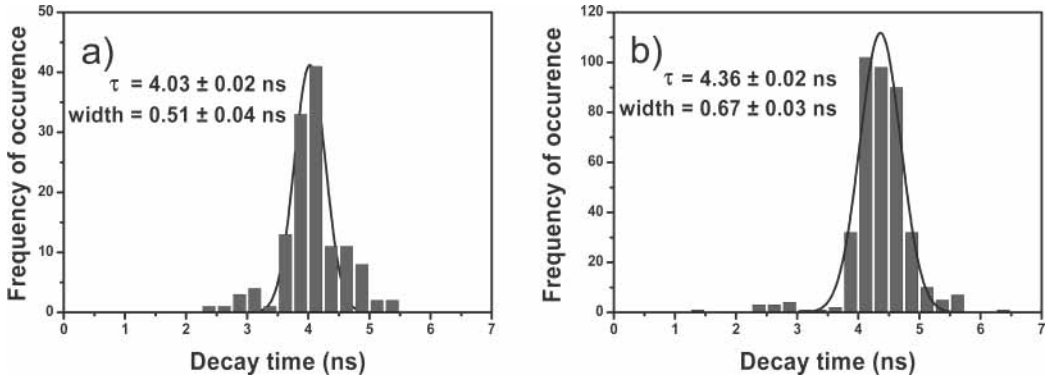

Figure 8. (a) Histogram of the decay values obtained from single molecules measurements of g1r2 in zeonex. (b) Histogram of the decay values obtained from single molecules measurements of g1r2 in PMMA.

Table 2 gives an overview of the values for the second off process. If we assume a lifetime of several milliseconds for this second off process then it is highly unlikely to find off events of several seconds. Therefore, this third and last off process, as can be seen in Figure 3c, must be of a different nature than the triplet and the second several milliseconds off process. The last process seems not dependent on the oxygen concentration because it occurs under normal atmospheric conditions and under nitrogen atmosphere. Also it can be found back in a PMMA and zeonex polymer matrix. Because of the low number of events, no statistic analysis could be performed.

The triplet related off events show the collective behavior of the chromophores. If one chromophore goes to the triplet state, this also quenches the fluorescence of the other chromophore as can be seen in Figure 3, parts a and d. This is an example of singlet−triplet annihilation like discussed above, demonstrated at the single molecule level.

Polarized Fluorescence Intensity Trajectories. Using polarized fluorescence intensity trajectories, we can demonstrate the energy hopping process at the single molecule level. The stepwise changes in fluorescence intensity in the transient as shown in Figure 3a can be explained by consecutive bleaching of the chromophores if the bleached chromophores do not act as a trap for the fluorescence. The parallel and perpendicular components of the fluorescence were recorded with two detectors (polarized transients). In this way, a trajectory of the degree of polarization (p) can be calculated using eq 8

$$p = \frac{I_{\mathrm{par}} - GI_{\mathrm{per}}}{I_{\mathrm{par}} + GI_{\mathrm{per}}} \tag{8}$$

where G is a factor that corrects for the different detection efficiencies of both detection channels. Figure 5 shows an example of the p trajectory of a g1r2 molecule embedded in zeonex. The p value stays constant even when changes in the fluorescence intensity in the trajectory occur. Hence, throughout the experiment, always the same chromophore is emitting and acts as the fluorescent trap from where emission occurs. This also indicates that after the stepwise bleaching, the bleached chromophore does not act as a trap for the fluorescence. A model

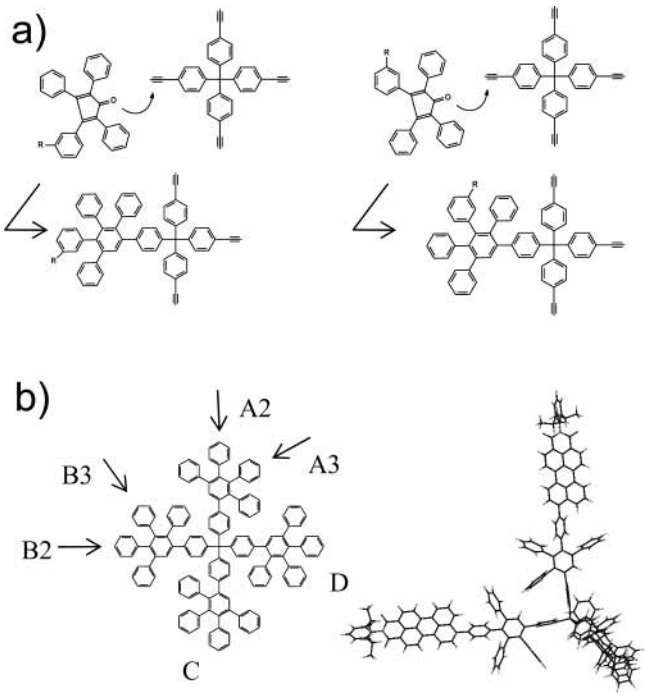

Figure 9. (a) Two possible modes of addition in the synthesis of the dendrimer. (b) 2D representation of where chromophores can be attached to the dendrimer and 3D representation of isomer 2B2A of compound **2**. The arrows indicate the possible places where the chromophore might be attached.

was proposed that emission occurs at all times only from the chromophore that is lowest in energy.[12] This implies that one chromophore is acting as a fluorescent trap while the other chromophore is communicating via Förster type energy hopping. On the basis of the overlap between the ensemble absorption and emission spectra and the calculated Förster radius of 4.78 nm, we can conclude that energy hopping is observed at the single molecule level.

Coincidence Measurements. Coincidence measurements[19,34,35] were done on single molecules of g1r2. The idea of these experiments was to see if g1r2 acts as a single emitter (one photon is emitted per pulse) or not (two photons are emitted per pulse) when excited with an intense laser pulse. Also this would demonstrate that the singlet−singlet annihilation process can be observed at the single molecule level. For a single chromophore, the probability of emitting two consecutive photons drops to zero for time intervals shorter than the excited state lifetime (referred to as antibunching in single molecule experiments).[35,36] After photon emission, a molecule must be re-excited and wait, on average, one fluorescence lifetime before another photon can be emitted. Therefore, a single chromophore compound like g1r1 cannot emit two photons simultaneously because the lifetime of the molecule is 4 ns and the pulse width of the laser is about 1.2 ps. If two independent chromophores are present in the diffraction limited excitation spot, they can emit each one photon. When these two photons generated by the same laser pulse are detected, they show up in the central peak of the interphoton arrival times histogram around 0 ns with a ratio of 0.5 with respect to the other peaks. In all other cases, interphoton arrival times are distributed around a multiple of the repetition rate, i.e., one peak every ∼123 ns. Figure 6 shows an example of a g1r2 molecule in zeonex. For clarity, only the central three peaks are given in Figure 6, parts a′ and a″. For the first intensity level in Figure 6a (corresponding to the letter a′) a ratio of 0.031 is found. A total of 34 counts were detected in the central peak and on average 1111 counts in the outer peaks. This is represented in Figure 6a′. The second level (corresponding to the letter a″) has a ratio of 0.021. A total of 9 counts were detected in the central peak and on average 435 counts in the outer peaks. This is represented in Figure 6a″. The absence of the central peak for a bichromophoric system can be explained by assuming a very efficient singlet−singlet annihilation process that is present in these systems when multiple excitations are introduced. One singlet state is excited to a higher excited singlet state, whereas the other one returns to the ground state. Therefore, the bichromophoric system acts as a single emitter, and no central peak is present in the coincidence measurement.

Spectral and Time-Resolved Single Molecule Experiments. To demonstrate that indeed the system is in the weak coupling regime and the Förster model is applicable, spectral and time-resolved single molecule experiments were performed. Single molecule fluorescence spectra of all recorded g1r2 molecules show a strong resemblance with the ensemble emission spectrum of g1r2 in toluene. This is in contrast with single molecule emission spectra of previously reported dendrimers where excimer-like spectra could be observed.[12,37] The absence of these unstructured, red shifted excimer-like spectra can be explained by the reduced flexibility of the core (sp^3 carbon atom instead of biphenyl core)[12] and difference in attachment of the chromophores (in para instead of meta position on the outer phenyl ring).[37] Both these aspects increase the average distance between the chromophores so that they can no longer form excimer-like entities. In Figure 7, parts a and b, a fluorescence intensity trajectory and a spectral run corresponding to this fluorescence intensity trajectory are given. In the first intensity level, the emission maximum is situated around 18 200 cm^{-1}. After 15.5 s, a jump to the second fluorescence intensity level can be observed, together with a blue shift of the emission spectrum to a maximum of 18 500 cm^{-1} on average. This blue shift is a generally observed trend as can be seen in Figure 7c. In this figure, the difference between the emission maxima of the last spectrum and the first spectrum of each recorded molecule is given. The histogram is mainly situated in the positive part, indicating a blue shift. A fraction however is situated in the negative part, indicating a red shift. The blue shift can be explained by assuming the emission comes from the chromophore that is lowest in energy and upon photobleaching of that chromophore, the next one that is higher in energy takes over the emission. An average value for the shift is 167 cm^{-1} to the blue side. This general trend to the blue can not only be explained by the loss of exciton splitting between the two chromophores when one chromophores photobleaches.[38,39] Another effect that can play a role is small energetic differences in the surrounding polymer matrix of the two chromophores. These energetic differences in the surrounding polymer can be dynamic and might explain the occasional red shift.

Single molecule decaytime measurements of g1r2 in zeonex and PMMA were done using circular polarized excitation light. For each molecule, each constant level was fitted and the resulting value was used in the histogram. From all of the recorded molecules, a histogram of the decay times was made. These histograms are given in Figure 8, parts a and b, respectively (the histogram in Figure 8a consists out of 133 data points, whereas the histogram in Figure 8b consists out of 392 data points). In Figure 8a, the histogram of the g1r2 molecules in zeonex is presented. We see a maximum at 4.03 ns which corresponds well to the ensemble value of 4 ns of g1r2 in toluene. Figure 8b represents the histogram of the g1r2

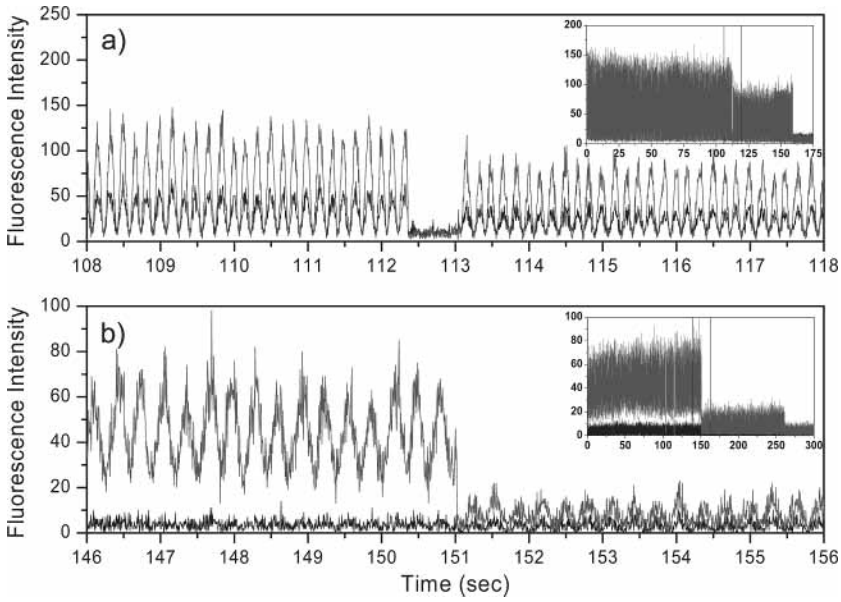

Figure 10. (a) Example of an IPM MFIT of a single g1r2 molecule. (b) Example of an IPMO MFIT of a single g1r2 molecule.

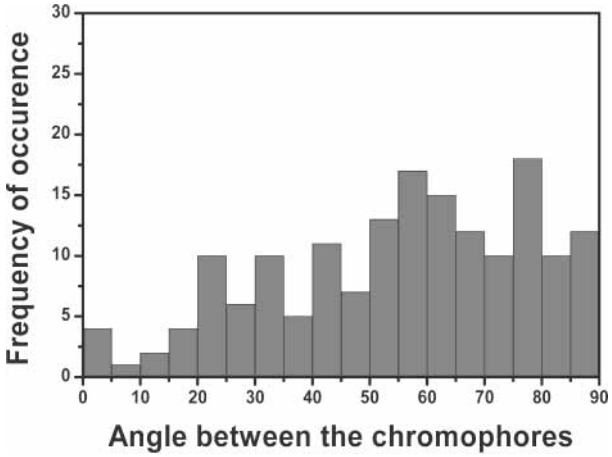

Figure 11. Experimentally obtained histogram of the projection of the angles between the chromophores in the $X-Y$ plane.

molecules in PMMA. Here we see a maximum that is situated at 4.36 ns. Also this is in good agreement with ensemble measurements done in ethyl acetate for g1r1 which resulted in a value of 4.43 ns.[40] For all of the determined decay times of g1r2 in both zeonex and PMMA, we do not find values around 8 ns confirming the absence of an excimer-like species.[12] The spectral and time-resolved single molecule measurements show that the specific attachment of the chromophores (in para position on the outer phenyl ring) avoids the formation of excimer-like species, and therefore, the Förster model is applicable.

Molecular Structure. One needs to take into account that a result of the asymmetric building blocks used in the Diels−Alder cycloaddition is that the attachment of the chromophores leads to structural isomers (Figure 9a).[37] If multiple chromophores are present, the excited state interaction between them might be different in the different structural isomers. Therefore, small differences can occur in the efficiencies of the previously discussed photophysical properties of one molecule to another. An example of possible structural isomers (2D) and one example of a 3D isomer of g1r2 is given in Figure 9b. As depicted in Figure 9b, there are four attachment places for the chromophores, and this normally results in four possible isomers. However, there is an asymmetry in the four polyphenyl branches resulting in two possible ways in which the two chromophores can be attached. The arrows indicate the possible substitution patterns of the chromophores in the different structural isomers. The four positions where a chromophore can be attached are A2, A3, B2, B3, C2, C3, D2, and D3 where A, B, C, and D represent the different branches and 2 and 3 the second or third phenyl group within each branch where a chromophore can be attached. For g1r1, however, the two different structural isomers that can be formed will show similar photophysical behavior.

Modulated Fluorescence Intensity Traces (MFIT). In these experiments, the direction of the linear polarized excitation light is being rotated at a frequency of several hertz. Because the chromophores will have a maximal absorption probability when the direction of the excitation light is parallel with the transition dipole moment of the chromophore, the rotation of the linear excitation light introduces a cosine squared modulation pattern of the fluorescence emission for a single absorbing chromophore. For two chromophores, the recorded MFITs can be classified in four groups depending on the pattern of the modulation in the first intensity level.[24]

The first class (6% of all recorded MFITs) is called in-phase modulation (IPM) which means that the modulation pattern in both detection channels is in phase and the modulation goes to the background. This occurs when the two chromophores are parallel, or when one of the chromophores is already bleached during the imaging process. In the case of very efficient energy transfer between the dyes, only one chromophore emits and consequently no phase shift between the two polarization channels is observed while there is an offset for nonparallel chromophores. This second class of patterns is called in-phase modulation with offset (IPMO) and has a contribution of 93% of all of the MFITs. The occurrence of IPMO pattern in a large fraction is only an indication for energy transfer but not a suitable means to distinguish uni- or two-directional transfer phenomena.[24] The third class is called no modulation (NM). Here no modulation was observed in the first level (1% of all MFITs). The fourth and last class is the out of phase modulation (OPM). In this class, there is a phase difference between the parallel and perpendicular channel present. This indicates that the two chromophores emit independently. This was as expected not observed. Figure 10 displays typical examples observed of two most important classes, the IPM and IPMO observed for

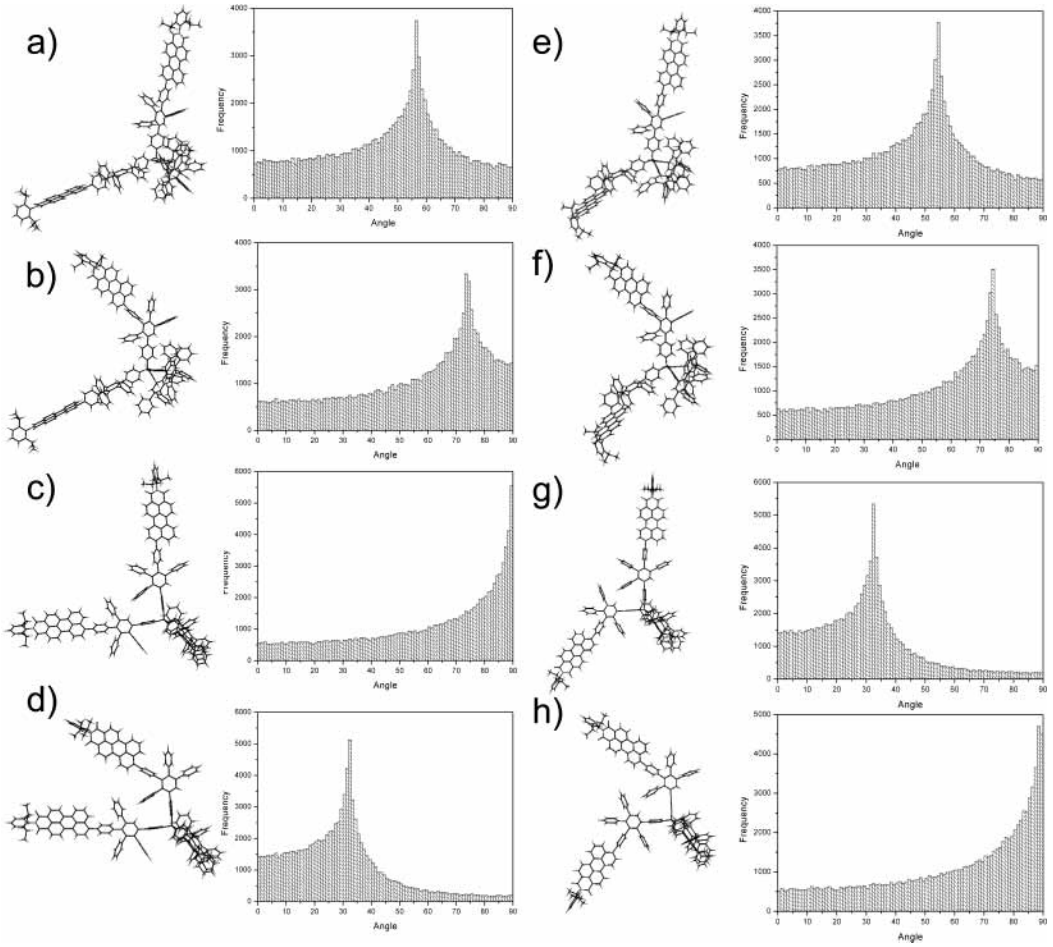

Figure 12. (a−h) Eight synthetically possible calculated structures together with a simulated histogram of the random projection of the angle between the chromophores in the $X-Y$ plane.

g1r2 molecules. From all IPMO molecules, we calculated the angle between the two chromophores and a histogram was constructed with all these values as can be seen in Figure 11. Because this is a projection of the angle in the experimentally observed $X-Y$ plane and not really the angle between the two chomophores, simulations were performed to construct histograms of the eight structural isomers such as the one that was experimentally observed.

This can be seen in Figure 12 where isomers a, b, e, and f correspond to the isomers of branch A and B, whereas the isomers c, d, g, and h correspond to isomers of branch A and C. The total number of isomers used on which calculations were done is therefore eight (isomers of branches A and B give the same results as isomers of branches C and D and are therefore omitted, the same is valid for isomers of branches A and C and isomers of branches B and D). Based on these structures, calculations of the projection of the angle between the chromophores in the $X-Y$ plane were done. This can be seen in Figure 12, where the projections of the eight different structural isomers that were calculated are presented.

For the structural isomers depicted in Figure 12, we find values of 56° (for all orientation angles given here, the complementary angle is also valid) for a, 74° for b, 90° for c, 33° for d, 56° for e, 74° for f, 33° for g, and 90° for h,and interchromophoric distances of 3.2 nm for a, 2.6 nm for b, 2.6 nm for c, 1.5 nm for d, 3.1 nm for e, 3.1 nm for f, 2.5 nm for g, and 2.3 nm for h. All of the results are projected into the [0°,90°] interval. It is clear from Figure 12 that, compared with the simulations, more than one isomer should be present to account for the peaks in the histogram. A peak can be seen between 75 and 80°. This peak might correspond to the structural isomer given in Figure 12, parts b and f. Between 50 and 60°, we find also a less well-defined peak that might correspond to the structural isomer in Figure 12, parts a and e. The combination of simulated and experimental data shows the presence of more than one isomer of g1r2, and a tentative attribution of the different maxima in the histogram to different isomers can be made.

Conclusions

In this paper, we studied a rigid bichromophoric dendritic system. The presence of structural isomers was demonstrated at the single molecule level by analyzing modulated fluorescence intensity trajectories. For this bichromophoric dendrimer, that can act as a model to understand more complex multichromophoric systems (especially FRET couples), we demonstrated the presence of several Förster type processes such as energy hopping, singlet−singlet annihilation, and singlet−triplet annihilation. Energy hopping and singlet−singlet annihilation were demonstrated at the ensemble and single molecule level, whereas singlet−triplet annihilation can only be demonstrated at the single molecule level showing that both methods are complementary and can lead to a better understanding of the photophysical processes in a multichromophoric system. Besides the triplet off processes, a hypothesis for the origin of the second off process was formulated, involving the possible formation of a radical anion.

Acknowledgment. T.V. thanks the I.W.T. for a doctoral fellowship. Financial support of the FWO, the DWTC through IUAP-5-03, and the Flemish Ministry of Education through GOA/1/2001 is gratefully acknowledged. Financial support through a Max Planck research award is gratefully acknowledged. M.C. acknowledges K. U. Leuven for a Postdoctoral fellowship, German Ministry of Education and Research. German Science Foundation (SFB625).

References and Notes

(1) Bopp, M. A.; Jia, Y. W.; Li, L. Q.; Cogdell, R. J.; Hochstrasser, R. M. *Proc. Natl. Acad. Sci. U.S.A.* **1997**, *94*, 10630.

(2) Bopp, M. A.; Sytnik, A.; Howard, T. D.; Cogdell, R. J.; Hochstrasser, R. M. *Proc. Natl. Acad. Sci. U.S.A.* **1999**, *96*, 11271.

(3) Cotlet, M.; Hofkens, J.; Habuchi, S.; Dirix, G.; Van Guyse, M.; Michiels, J.; Vanderleyden, J.; F. C. De Schryver *Proc. Natl. Acad. Sci. U.S.A.* **2001**, *98*, 14398.

(4) VandenBout, D. A.; Yip, W. T.; Hu, D. H.; Fu, D. K.; Swager, T. M.; Barbara, P. F. *Science* **1997**, *277*, 1074.

(5) Yu, J.; Hu, D.; Barbara, P. F. *Science* **2000**, *289*, 1327.

(6) Huser, T.; Yan, M.; Rothberg, L. J. *Proc. Natl. Acad. Sci. U.S.A.* **2000**, *97*, 11187.

(7) Hollars, C. W.; Lane, S. M.; Huser, T. *Chem. Phys. Lett.* **2003**, *370*, 393.

(8) Sarzi Sartori, S.; De Feyter, S.; Hofkens, J.; Van der Auweraer, M.; De Schryver, F. C.; Brunner, K.; Hofstraat, J. W. *Macromolecules* **2003**, *36*, 500.

(9) Weil, T.; Wiesler, U. M.; Herrmann, A.; Bauer, R.; Hofkens, J.; De Schryver, F. C.; Müllen, K. *J. Am. Chem. Soc.* **2001**, *123*, 8101.

(10) Maus, M.; De, R.; Lor, M.; Weil, T.; Mitra, S.; Wiesler, U. M.; Herrmann, A.; Hofkens, J.; Vosch, T.; Müllen, K.; De Schryver, F. C. *J. Am. Chem. Soc.* **2001**, *123*, 7668.

(11) De Belder, G.; Jordens, S.; Lor, M.; Schweitzer, G.; De, R.; Weil, T.; Hermann, A.; Wiesler, U. M.; Müllen, K.; De Schryver, F. C. *J. Photochem. Photobiol. A: Chem.* **2001**, *145*, 61.

(12) Hofkens, J.; Maus, M.; Gensch, T.; Vosch, T.; Cotlet, M.; Köhn, F.; Herrmann, A.; Müllen, K.; De Schryver, F. C. *J.* Am. Chem. Soc. **2000**, *122*, 9278.

(13) Aloisi, G. G.; Elisei, F.; Latterini, L. J. *Chem. Soc. Faraday Trans.* **1992**, *88*, 2139.

(14) Carmichael, I.; Hug, G. L. *J. Phys. Chem. Ref. Data* **1986**, *15*, 1.

(15) Schweitzer, G.; Xu, L.; Craig, B.; De Schryver, F. C. *Optic. Commun.* **1997**, *142*, 283.

(16) Eggeling, C.; Fries, J. R.; Brand, L.; Gunther, R.; Seidel, C. A. M. *Proc. Natl. Acad. Sci. U.S.A.* **1998**, *95*, 1556.

(17) Cotlet, M.; Hofkens, J.; Maus, M.; De Schryver, F. C. *Fluorescence spectroscopy, Imaging and probes: new tools in chemical, physical and life sciences*; Springer-Verlag: Heidelberg, 2002.

(18) Maus, M.; Cotlet, M.; Hofkens, J.; Gensch, T.; De Schryver, F. C.; Schaffer, J.; Seidel, C. A. M. *Anal.* Chem. **2001**, *73*, 2078.

(19) Weston, K. D.; Dyck, M.; Tinnefeld, P.; Müller, C.; Herten, D. P.; Sauer, M. *Anal. Chem.* **2002**, *74*, 5342.

(20) Weston, K. D.; Buratto, S. K. *J. Phys. Chem. A* **1998**, *102*, 3635.

(21) Weston, K. D.; Carson, P. J.; DeAro, J. A.; Buratto, S. K. *Chem. Phys. Lett.* **1999**, *308*, 58.

(22) Jackel, F.; De Feyter, S.; Hofkens, J.; Köhn, F.; De Schryver, F. C.; Ego, C.; Grimsdale, A.; Müllen, K. *Chem. Phys. Lett.* **2002**, *362*, 534.

(23) Ying, L.; Xie, S. J. *Phys. Chem. B* **1998**, *102*, 10399.

(24) Gensch, T.; Hofkens, J.; Köhn, F.; Vosch, T.; Herrmann, A.; Müllen, K.; De Schryver, F. C. *Single Mol.* **2000**, *2*, 35.

(25) Förster, T. *Ann. Phys.* **1948**, *2*, 55. Translated by R. S. Knox, Department of Physics and Astronomy, University of Rochester, Rochester, NY.

(26) Lakowicz, J. R. *Principles of fluorescence spectroscopy*, 2nd ed.; Kluwer Academic/Plenum Publishers: New York, 1999; p 369.

(27) De Belder, G.; Schweitzer, G.; Jordens, S.; Lor, M.; Mitra, S.; Hofkens, J.; De Feyter, S.; Van der Auweraer, M.; Herrmann, A.; Weil, T.; Müllen, K.; De Schryver, F. C. *ChemPhysChem* **2001**, *2*, 1.

(28) Jordens, S.; De Belder, G.; Lor, M.; Schweitzer, G.; Van der Auweraer, M.; Weil, T.; Herrmann, A.; Wiesler, U. M.; Müllen, K.; De Schryver, F. C. *Photochem. Photobiol. Sci.* in press.

(29) Hofkens, J.; Schroeyers, W.; Loos, D.; Cotlet, M.; Köhn, F., Vosch, T.; Maus, M.; Herrmann, A.; Müllen, K.; Gensch, T.; De Schryver, F. C.; *Spectrochim. Acta Part A* **2001**, *57*, 2093.

(30) The oxygen permeability constant of PMMA is 20 times lower than that of low-density polyethylene (we assume this has a similar oxygen permeability as zeonex). *Polymer Handbook*, 3rd ed.; Brandrup, J. B., Immergat, E. H., Eds.; John Wiley and Sons Inc.: New York, 1989; p VI-437.

(31) Lor, M.; Thielemans, J.; Viaene, L.; Cotlet, M.; Hofkens, J.; Weil, T.; Hampel, C.; Müllen, K.; Verhoeven, J. W.; Van der Auweraer, M.; De Schryver F. C. *J. Am. Chem. Soc.* **2002**, *124*, 9918.

(32) Lee, S. K.; Zu, Y.; Herrmann, A.; Geerts, Y.; Müllen, K.; Bard, A. J. *J. Am. Chem. Soc.* **1999**, *121*, 3513.

(33) Lor, M.; Jordens, S.; De Belder, G.; Schweitzer, G.; Fron, E.; Viaene, L.; Cotlet, M.; Weil, T.; Müllen, K.; Verhoeven, J. W.; Van der Auweraer, M.; De Schryver, F. C. *Photochem. Photobiol. Sci.* **2003**, *2*, 501.

(34) Tinnefeld, P.; Muller, C.; Sauer, M. *Chem. Phys. Lett*. **2001**, *345*, 252.

(35) Tinnefeld, P.; Weston, K. D.; Vosch, T.; Cotlet, M.; Hofkens, J.; De Schryver, F. C.; Sauer, M. *J. Am. Chem. Soc*. **2002**, *124*, 14310.

(36) Basche, T.; Moerner, W. E.; Orrit, M.; Talon, H. *Phys. Rev. Lett.* **1992**, *69*, 1516.

(37) Vosch, T.; Hofkens, J.; Cotlet, M.; Köhn, F.; Fujiwara, H.; Gronheid, R.; Van Der Biest, K.; Weil, T.; Herrmann, A.; Müllen, K.; Mukamel, S.; Van der Auweraer, M.; De Schryver, F. C. *Angew. Chem., Int. Ed.* **2001**, *40*, 4643.

(38) CEO−INDO/S (Collective Electronic Oscillators-Intermediate Neglect of Differential Overlap/ Spectroscopic) calculations done on a similar dendrimer structure bearing four chromophores show that values ranging from 10 to 60 cm^{-1} (at zero Kelvin and in a vacuum) can be found for the coupling constant among the chromophores in the different structural isomers. Unpublished results.

(39) Christ, T.; Petzke, F.; Bordat, P.; Herrmann, A.; Reuther, E.; Müllen, K.; Basché J. *Lumin.* **2002**, *98*, 23.

(40) Unpublished results.